

SMALL ANGLE NEUTRON SCATTERING APPLICATIONS IN FUEL SCIENCE

P. Thiyagarajan
IPNS Division
George D. Cody, Jerry E. Hunt and Randall E. Winans
Chemistry Division
Argonne National Laboratory
Argonne, IL 60439.

Keywords: SANS Asphaltene Coal

INTRODUCTION

Small angle neutron scattering (SANS) is a versatile technique¹, extensively used in condensed matter research, spanning the scientific fields including polymer science, metallic alloys, magnetic materials, porous materials, ceramics, composites, structural biology and colloidal systems of industrial and technological importance. SANS is useful to study both solid and liquid systems to obtain the size, morphology, molecular weight, particle size distribution in a size range of 10 to 1000 Å, as well as to study the phenomena such as phase separation, crystallization etc. In the presence of inter-particle interactions (e.g. ionic micelles) this will yield information on the surface potentials (e.g. surface charge density) of the colloids².

Three properties of neutrons make SANS to be unique and the information complementary to other techniques. The scattering cross-sections of the elements do not depend on their atomic number, but vary between the isotopes³; e.g., $b_H = -0.3740 \times 10^{-12} \text{cm}$ and $b_D = 0.6674 \times 10^{-12} \text{cm}$. This permits investigations of systems containing hydrogen (polymers, biological macromolecules, micelles, coals, asphaltene) and multicomponent systems (clay-polymer composites, virus, microemulsions, coals). The high penetration of cold neutrons is valuable for the study of bulk materials under a variety of conditions, such as a wide range of temperature, magnetic field, pressure, shear etc. The magnetic moment of neutrons permits them as a powerful probe for the study of magnetic materials.

The SANS experiments can be carried out at either reactor facilities (e.g. ORNL, NIST, ILL-France), or at Pulsed Neutron Sources (e.g. ANL, ISIS-Great Britain). The neutron beams, usually, have circular cross-section with a diameter of 8-12mm, and the sample thicknesses are typically 1-5mm, depending on the chemical composition of the sample. Majority of SANS experiments require data in a wide q ($q = 4\pi \sin\theta/\lambda$, where θ is the half the scattering angle and λ is the wavelength of the neutrons) range, in order to carry out analysis on morphology, fractal dimension, particle size distribution, phase separation etc. To measure data in a wide q range at the SANS instruments at reactors, one has to repeat the experiments 2 to 3 times by changing the sample-to-detector distance or the wavelength of the neutrons or both. The SANS instruments at the pulsed neutron sources, on the other hand, yield data in a wide q range in a single measurement, by using neutrons with a wide range of wavelengths which are determined by time-of-flight techniques. This may serve as an advantage for studying systems which cannot be exactly reproduced for the repetitive measurements. In this paper we discuss briefly a few fundamental principles of SANS and demonstrate the technique with a few examples.

BASIC PRINCIPLES

A number of reviews^{4,5,6} describe the basic principles of small angle scattering and hence we only give relevant formulae useful for obtaining the structural information. Briefly, the intensity of the scattered neutrons, $I(q)$, in the low q region is determined by the number density of particles, n , the distance correlations due to time-averaged position vectors of the atoms within a particle [intra-particle structure factor, $P(q)$] and those due to the distribution of particles [inter-particle structure factor, $S(q)$] within the sample volume.

$$I(q) = n P(q) S(q) \quad (1)$$

In dilute systems $S(q)$ tend to oscillate around 1.0 in the low q region and the measured $I(q)$ is determined essentially by $P(q)$. Analysis of the measured $I(q)$ for dilute systems will yield direct information on the structural properties of the particles, in terms of size and shape. If the data is calibrated to be on an absolute scale, additional information such as molecular weight and volume can also be obtained. In the absence of inter-particle interactions the differential scattering cross-section can be written as

$$I(q) = k \int (\rho_s - \rho_m) e^{iqr} d^3r \quad (2)$$

where ρ_s and ρ_m are the scattering length densities (scattering length per unit volume) for the particle and the matrix, and the k includes all the constants to place the data on an absolute scale. Table I contains scattering length densities ($\rho = \sum b \cdot N_A \cdot d/M$, where b is the scattering length³, N_A is the Avogadro's number, d is the physical density and M is the molecular weight) for a number of normal and per-deuterated solvents. At low q region, equation 2 reduces to a simple form, Guinier equation⁴,

$$I(q) = I(0) \exp(-q^2 R_g^2/3) \quad (3)$$

$$I(0) = n v^2 (\rho_s - \rho_m)^2 \quad (4)$$

In eq. 3, R_g is known as the radius of gyration of the particle and v in eq. 4 is the volume of the solvent excluded by the particles. This is defined as the root-mean square value of all the pair-wise distances from the centroid of the scattering volume and this parameter does not specify the shape. In the case of monodisperse system, R_g can be used to determine the dimensions of the particles, provided the shape is known. In the case of spherical particles $R_g = \sqrt{3/5}$ radius. A plot of $\text{Ln} I(q)$ vs. q^2 (Guinier plot) will yield a straight line in the q region where $q R_g \leq 1.0$. The absolute slope of the straight line can be used to determine the R_g and the y-intercept yields $I(0)$ which can be used to determine the molecular weight of the particle. In the case of polydisperse systems the measured R_g is the z-averaged value given by $R_g^2 = \sum N_i M_i^2 R_{g_i}^2 / \sum N_i M_i^2$ and the molecular weight from $I(0)$ is the weight-averaged value. It can be seen from eq. 4 that the magnitude of $I(0)$ can be manipulated by changing either the scattering length density of the solute, ρ_s , or the solvent, ρ_m , and can be made zero by exactly matching these two parameters. This method is called contrast variation⁷ which can be done by changing the deuteration levels of either the solute or solvent. In the case of binary system the contrast variation method can be used to determine $I(0)$ at different ρ_m values and a plot of $\sqrt{I(0)}$ vs ρ_m will give a straight line whose slope is proportional to the solvent excluded volume, v (see eq. 4) and the x-intercept gives ρ_s value. The value in turn can be used to determine the partial specific volume of the particle provided the chemical composition of the constituents is known. The contrast matching technique has been used to advantage in the case of coals. The composition and the density of the coals is such that its scattering length density is similar to the scattering length density of perdeuterated toluene (see Table I). If coal is imbibed in the perdeuterated toluene then for neutrons the particulate region of the coal and the solvent filling the accessible pores resemble as a system of uniform scattering length density. Hence the scattering from the pores accessible to the solvent will be negligible. However if there exists pores inaccessible to the solvent then they will produce SANS signals. Thus SANS can be used to characterize the closed pores in coals as well as other porous materials⁸. Such manipulation has also been done to see the effects of confined space on the phase separation in binary solvents⁹ and micellization.

As mentioned earlier, the low q region gives the size parameter, R_g , but delineation of the shape information requires data in a wide q region. The $\log(I)$ vs. $\log(q)$ plots yield important information on the probable shapes. In the case of infinitely long particles the scattering signal in the low q region is convoluted by a powerlaw of q^{-1} . In the case of sheet like particles the scattering signal in the low q region is convoluted by a powerlaw of q^{-2} . Thus the measured differential scattering cross-sections for the rod and a sheet, respectively, are given by

$$I(q) = q^{-1} \exp(-q^2 R_c^2/2) \quad (5)$$

$$I(q) = q^{-2} \exp(-q^2 R_t^2) \quad (6)$$

These equations can be used to obtain the cross-sectional radius of gyration, R_c , of the rod-like particle from a modified Guinier plot⁵ for a rod, $\text{Ln} [q \cdot I(q)]$ vs. q^2 and the thickness factor, R_t , of the lamellar particle can be obtained from a modified Guinier plot for a sheet, $\text{Ln} [q^2 \cdot I(q)]$ vs. q^2 . The radius of the rod can be obtained by multiplying R_c by $\sqrt{2}$, and the thickness of the sheet can be obtained by multiplying the R_t by $\sqrt{12}$. The y-intercepts in these plots can be used to obtain the mass per unit length and mass per unit area respectively.

For obtaining information on the morphology of the particles, the data in the whole q region can be modelled by using the form factors for shapes such as sphere, ellipsoid, cylinder, random coil etc., and obtain the size parameters best describing the scattering signal. Form factors for several known geometries are available in Guinier and Fournet (1955)⁴

In the case of self-similar aggregates the scattering signals exhibit powerlaw behavior in a wide q region. The $\log(I)$ vs $\log(q)$ plots can be fitted in the linear regions and the absolute values of the slope can be used to describe the system in terms of fractal dimensions¹⁰⁻¹². If the absolute value of the slope is a fraction in the region of 1-3, then the system is a mass fractal and the magnitude tells about the packing density of the fractal objects. If the fractal objects are formed through aggregation then it is possible to delineate the kinetics of aggregation. For example if the absolute value of the slope is around 1.7 then the cluster-cluster aggregation model may explain the aggregation mechanism, and if it is around 2.5 then it could be due to diffusion limited aggregation. If the absolute value of the slope is between 3-4 then the system is quite large and the system may be a surface fractal. A value close to 4 corresponds to a smooth surface and that close to 3 implies a particles with a rough surface.

The scattering signal in the case of polydisperse systems cannot easily be fitted with either the form factor of known geometrical objects or at times it may not exhibit linear curves in the Guinier plot [$\ln I(q)$ vs q^2]. If the measured scattering data contains data in the q region where $qR_g \leq 1.0$ such that R_g is the largest particle size then unique information on the particle size distribution can be obtained by using maximum entropy technique. If the particles are too large and the data cannot be measured to very low q values fulfilling the relationship $qR_g \leq 1.0$, then it may not be possible to get the correct particle size distribution. The pore size distribution in coals is quite wide and the pores are quite large and hence the scattering techniques cannot give the correct pore size distribution for coals.

EXPERIMENTAL

We have conducted a number of SANS experiments on coals, coal macromolecules and asphaltenes at the Small Angle Diffractometer (SAD) at the Intense Pulsed Neutron Source of Argonne National Laboratory. This instrument uses neutrons produced in pulses by spallation due to the deposition of 450 MeV protons on a depleted uranium target, followed by a solid methane moderator (22 K) yielding a wavelength range of 1 to 14 Å. Detection of scattered neutrons was accomplished with an area sensitive, gas-filled proportional counter, and the wavelength of the scattered neutrons was determined by their times-of-flight. The accessible q range using SAD is from 0.005 to 0.25 \AA^{-1} in a single measurement. The samples at ambient to 100 C were measured in Suprasil cells, while the high temperature measurements were done in a stainless steel cell.

EXAMPLES

Coals are complex materials and a variety of techniques have been applied to understand their chemical and physical structures. Scattering studies on coals have brought out the fractal nature of the network structure¹² and the structural modifications occurring due to solvents such as pyridine. SANS showed that Pittsburgh #8 in C_5D_5N swelling is due to the breaking of the hydrogen bonded network of coal structure¹³. In order to gain a better understanding of the coal structure we took an approach to study the pyridine-extracted species¹⁴ in deuteriopyridine as well as the extracts with their acidic groups methylated. The scattering behavior of both neat and O-methylated extracts of APCS #3 (5 wt.% in C_5D_5N) is shown in Fig. 1a and the Guinier plot for the neat sample is shown in Fig. 1b. The slope of the fitted line in Fig. 1b gives an R_g of $41 \pm 3 \text{ \AA}$ and $I(0) = 0.01 \text{ cm}^2 \cdot \text{mg}^{-1}$ which corresponds to a molecular weight of 6365 daltons and a solvent excluded volume of 9000 \AA^3 . This clearly shows that the macromolecule is not a solid sphere, rather a random coil. The data thus can be fitted well with the form factor for a random coil and the fit is also shown in Fig. 1 for the neat sample. The R_g value from the fit is consistent with that from Guinier analysis. The O-methylated macromolecules exhibit a powerlaw behavior in the low q region with an absolute slope of -1.7 (Fig. 1a). However the scattering behavior is similar in the q region above 0.03 \AA^{-1} . This indicates that the particles are similar in both neat and O-methylated samples, however they aggregate further in the O-methylated sample. The blocking of the hydrogen bonding interactions between the macromolecular surface and deuteropyridine leads to large network structures resembling a system aggregated due to cluster-cluster aggregation. The size of the smaller cluster is around 70 \AA . We observed that the differences between the neat and O-methylated cases decreases with decreasing in rank of the coals, however the network structures seem to be more dense than seen in the case of APCS #3 in C_5D_5N .

Another system in the fuel chemistry which is quite complex and widely studied is the asphaltenes. We carried out SANS studies on heptane precipitated asphaltenes¹⁵ from Maya vacuum resid in deuteriated 1-methylnaphthalene (d10-1MN) in a wide temperature range of 20 to 400 C. This study showed that a 5 wt.% asphaltene solution in d10-1MN at ambient temperatures form large colloidal systems, but they break down with increasing temperature. To compare the behavior of extracted coal macromolecules and asphaltene colloids we have shown the temperature effect on R_g and $I(0)$ values in Figs. 2a and 2b respectively. It can be seen that at 20C the size and $I(0)$ for the asphaltene colloids in d10-1MN are larger than those for the pyridine extracted coal macromolecules in C_5D_5N . With increase in temperature the asphaltene colloids become smaller than the coal macromolecules (Fig. 2a). However the $I(0)$ values, which are directly proportional to the solvent excluded volume of the particles and the contrast, continue to be larger than the coal macromolecules. The larger $I(0)$ values for the asphaltenes (smaller size) suggest that the asphaltene colloids may be more densely packed than the coal macromolecules in C_5D_5N . This can be confirmed with contrast variation studies on asphaltenes in organic solvents and such studies are in progress. Our studies on asphaltenes¹⁵ showed that they have a rod shape with a radius around 18 \AA , but with varying lengths depending on the temperature. We used modified Guinier analysis (Fig. 3a) to obtain the cross-sectional radius of the particle and MaxEnt analysis for the polydispersity (Fig. 3b).

CONCLUSIONS

In the field of fuel chemistry we encounter several systems which are quite complex as well as multicomponent in nature (crude oil). A wide range of physical and chemical methods have

been used to understand these systems and we are still far from complete understanding. For example coals have been studied in pure solid to chemically modified states. Since chemical modification and/or solvent extraction result in a number of different systems, it would be very important to understand the products in terms of their colloidal properties as a function of the type of solvent used to disperse them, as well as other physical conditions. Such knowledge will be helpful in the design of processing techniques. Another area of research where SANS can be useful is in the characterization of synthetic and modified clays^{16,17} which are being developed for processing in the petroleum industry. The major limitations for performing SANS experiments are the nonavailability/high cost of certain deuteriated solvents and the paucity of beam time at the neutron scattering centers.

ACKNOWLEDGEMENT

This work benefited from the use of the Intense Pulsed Neutron Source, ANL funded by the Office of Basic Energy Sciences, Division of Materials Science, U.S. Department of Energy under contract # W-31-109-ENG-38. This work was done under the auspices of U.S. DOE, BES-Division of Chemical Sciences under the same contract.

REFERENCES:

- 1) L.A. Feigin & D. I. Svergun (1987) Structure Analysis by Small Angle X-ray and Neutron Scattering, Plenum Press, New York.
- 2) S. H. Chen, E. Y. Sheu, J. Kalus & H. Hoffmann (1988) J. Appl. Cryst. 21, 751-769.
- 3) V. F. Sears, Neutron Scattering Lengths and Cross sections. In K. Skold & D. L. Price (ed) Neutron Scattering Methods of experimental Physics, R. Celotta & J. Levine (Series ed) 23A, 521-549) Academic Press, Inc, New York.
- 4) A. Guinier & G. Fournet (1955) Small Angle Scattering, Wiley, New York.
- 5) O. Glatter & O. Kratky (1982) Small Angle X-ray Scattering, Academic Press, New York.
- 6) G. D. Wignall, (1987) In Encyclopedia of Polymer Science and Engineering, 2nd ed. Vol.10 112-184, Wiley, New York.
- 7) H.B. Stuhmann & A. Miller (1978) Small ANgle Scattering of Biological Molecules, J. Appl. Cryst. 11, 325-345.
- 8) P.J. Hall, M.M. Antxustegi & J.M. Calo (1994) (Private Communication to P. Thiyagarajan)
- 9) M.Y. Lin, S.K. Sinha, J.M. Drake, X.-I. Wu, P. Thiyagarajan & H.B. Stanley (1994) Phys Rev Letters, 72, 2207-2210.
- 10) J. Feder (1988) *Fractals*, Plenum Press, New York.
- 11) T. Freltoft, J. K. Kjems & S.K. Sinha (1986) *Physical Rev. B*, 33, 269
- 12) H.D. Bale & P.W. Schmidt (1984) *Phys. Rev. Lett.*, 53, 596.
- 13) R.E. Winans & P. Thiyagarajan (1988) *Energy & Fuels* 2, 356
- 14) G.D. Cody, P. Thiyagarajan, R. E. Botto, J. E. Hunt & R.E. Winans (1994) *Energy and Fuels* 8, 1370-78.
- 15) P. Thiyagarajan, J.E. Hunt, R.E. Winans, K.B. Anderson & J.T. Miller (1995) *Energy and Fuels* (In Press)
- 16) K.A. Carrado, P. Thiyagarajan, R.E. Winans & R.E. Botto (1991) *Inorganic Chemistry*, 30, 794-799.
- 17) A. Moini, T.J. Pinnavaia, P. Thiyagarajan & J.W. White (1988) *J. Appl. Cryst* 21, 840-842.

TABLE I
Neutron Scattering Length Densities (ρ)

System	Chemical formula	Density(g/cm ³)	$\rho(10^{10}\text{cm}^{-2})$
Benzene	C ₆ H ₆	0.8786	1.18
Benzene-d6	C ₆ D ₆	0.950	5.43
Cyclohexane	C ₆ H ₁₂	0.7786	-0.277
Cyclohexane-d12	C ₆ D ₁₂	0.89	6.678
Methanol	CH ₃ OH	0.7914	-0.373
Metanol-d4	CD ₃ OD	0.89	5.81
1-methylnaphthalene	C ₁₁ H ₁₀	1.02	1.54
1-methylnaphthalene-d10	C ₁₁ D ₁₀	1.1	6.08
Pyridine	C ₅ H ₅ N	0.9819	1.79
Pyridine-d5	C ₅ D ₅ N	1.05	5.71
Toluene	C ₆ H ₅ CH ₃	0.8669	0.94
Toluene-d8	C ₆ D ₅ CD ₃	0.94	5.64
Water	H ₂ O	1.0	-0.56
Water-d2	D ₂ O	1.105	6.358
polycrystalline carbon		1.4	5.6

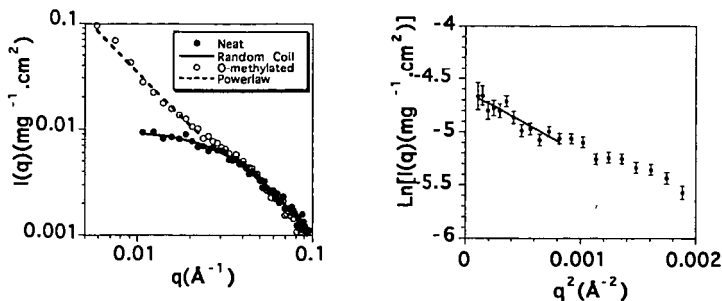


Fig. 1a: SANS of APCS #3 in $\text{C}_5\text{D}_5\text{N}$ (●), solid line is the fit for a random coil. Data for O-methylated extracts (○), dotted line is the powerlaw fit. Fig. 1b: Guinier plot for the pyridine extracts from APCS #3 in $\text{C}_5\text{D}_5\text{N}$. The size of error bars is smaller than the size of the symbols.

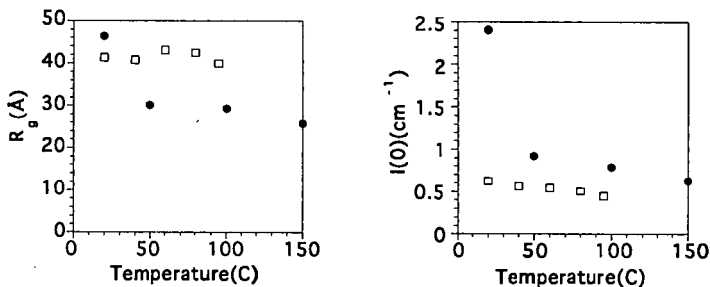


Fig. 2a: Temperature effect on the R_g of the 5 wt% APCS #3 macromolecules in $\text{C}_5\text{D}_5\text{N}$ (square) and 5 wt.% asphaltenes in $\text{C}_{11}\text{D}_{10}$ (filled o). Fig 2b: Temperature effect on the $I(0)$ of the APCS #3 pyridine extracts in $\text{C}_5\text{D}_5\text{N}$ (square) and 5 wt.% asphaltenes in $\text{C}_{11}\text{D}_{10}$ (o). The size of error bars is smaller than the size of the symbols.

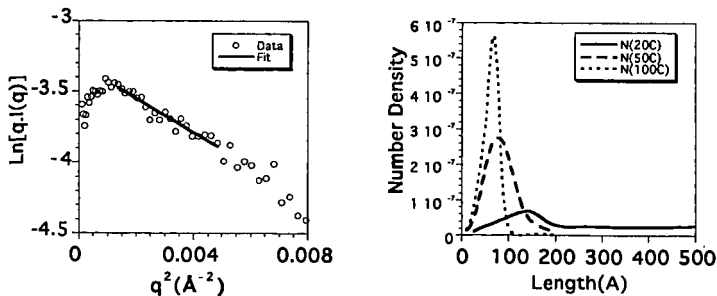


Fig. 3a: Modified Guinier plot for the 5 wt.% asphaltenes in $\text{C}_{11}\text{D}_{10}$ at 20°C. The size of error bars is smaller than the size of the symbols. Fig. 3b: Length distribution for the 5 wt.% asphaltenes in $\text{C}_{11}\text{D}_{10}$ as a function of temperature (radius of the rods is 18 \AA). 20C (solid line), 50C (dashed line), 100C (dotted line).